Identifying Mutations That Affect the TFIIIC-Dependent Pathway of Heterochromatin Boundary Function in *S. pombe.*

Robert K. Roth
Colorado College
MB499
8, March 2018

Thesis Advisor: _____
Jennifer Garcia, Ph.D.

*Second Reader:*_____
Darrell Killian, Ph.D.

Title**: Identifying Mutations That Affect the TFIIIC-Dependent Pathway of Heterochromatin Boundary Function in *S. pombe.***

Abstract:

Heterochromatin boundary elements inhibit the spread of repressive histone methylation through gene coding regions to prevent the silencing of nearby genes. Two parallel and redundant pathways are responsible for the function of heterochromatin boundaries in the fission yeast, *Schizosacchromyces pombe*; A pathway that involves TFIIIC, a transcription factor that associates with specific DNA elements, and a pathway that involves Epe1, a Jmjc domain-containing protein enriched at heterochromatin boundaries. Although TFIIIC and Epe1 are known to regulate heterochromatin boundaries, their mechanisms of action are still relatively unknown. To elucidate the proteins involved in the TFIIIC-dependent pathway of boundary function, chemical mutagenesis was employed using a reporter strain that reads out boundary function and lacks the Epe1-dependent boundary pathway. Mutants that exhibited impaired TFIIIC-dependent boundary function were sequenced to identify individual point mutations in four unique genes, *sda1*, *cog5, dpb2*, and *byr3*. To test if these genes play a role in TFIIIC-dependent boundary function, a CRISPR/Cas9 system was engineered to target wildtype genes in the Epe1-deficient reporter strains and reintroduce the identified mutations. The CRISPR/Cas9 plasmids were successfully amplified with sgRNA inserts capable of targeting Cas9 to *sda1+, cog5+, dpb2+,* and *byr3+*. The plasmids and sgRNA sequences were confirmed by CspCI restriction enzyme digest and Sanger sequencing. These plasmids will be transformed into *S. pombe* to generate reporter strains harboring each mutation, which can be used to verify if these mutations impair TFIIIC-dependent boundary function.

Introduction:

The chromosomes of many complex eukaryotic organisms are organized into strictly defined transcriptionally active and transcriptionally silent regions which are termed euchromatic and heterochromatic, respectively. Euchromatin is accessible to proteins such as transcription factors and transcriptional machinery recruited to these DNA regions by promoters, silencers, and enhancers, and is usually gene rich. Heterochromatin regions are highly-condensed portions of the genome, typically repetitive in sequence and inaccessible to transcriptional machinery. Heterochromatin functions in gene regulation by silencing regions of the genome and maintains the chromosome integrity by preventing repetitive, non-coding DNA sequences from recombining with transcriptionally active regions of the genome (Grewal and Jia 2007). The entirety of the eukaryotic genome, both euchromatin and heterochromatin, is organized into nucleosomes, a structure consisting of DNA tightly wrapped around eight histone proteins.

The histone proteins that constitute a nucleosome can be chemically modified, allowing for the organization and modification of the chromatin structure at certain regions of DNA. The specific modifications are performed by histone transferases, which transfer methyl, acetyl, ubiquitin, and small ubiquitin-like modifier (SUMO) groups to the amino acid residues of histone proteins (Smith and Denu 2009; Hay 2005). These histone modifications allow for regions of the genome to become more accessible, and as a result more readily available to transcriptional machinery, or more tightly packaged, and inaccessible. In addition, acetylated and methylated histones are recognized by specific proteins that modify or maintain the chromatin structure in that specific region of DNA. In the case of repressive histone methylation, the heterochromatin protein 1 (HP1) family of proteins bind to methylated histones and recruit a histone methyltransferase causing the spread of heterochromatin across a region of DNA in a sequence independent manner (Johnson, Cao, and Jacobsen, 2002). The ability of heterochromatin to spread is vital to many processes such as X-chromosome silencing (Tamaru 2010). If unchecked, the spread of heterochromatin can span thousands of kilobases and can thus effect other distal genes (Grewal and Moazed 2003).

Due to this sequence independent manner of heterochromatin spread, the regions of heterochromatin must be stringently controlled so that they do not spread into neighboring gene coding regions. Therefore, boundary elements have developed as a mechanism to contain the spread of heterochromatin. These boundary elements act to contain the spread of heterochromatin to the specific heterochromatic regions of DNA, while maintaining a euchromatic state for neighboring regions of the genome. The proper function of a heterochromatin boundary prevents the spread of silencing and can become a serious issue when tumor suppressor genes or important cell cycle maintenance genes are consequently effected. Maintaining the functional boundary between transcriptionally active genes and other areas of transcriptional silencing has implications in human cancers and cellular differentiation events, as well (Nguyen et al 2010; Ueda et al. 2014).

To experiment with and gain insight into the mechanisms of heterochromatin spread and the boundary elements that prevent its spread, we employed the model

organism, *S. pombe.* *S. pombe* is utilized to study boundary function because it exhibits a mechanism for heterochromatin formation and boundary function that is highly conserved across higher eukaryotes. The specific marker for repressive histone methylation and therefore, heterochromatin, is the methylation of lysine residue 9 on the histone protein H3 (H3K9me) (Yan and Boyd 2006). This mark is found within regions of the genome and allows for the recruitment of other proteins that modify chromatin structure and even induce the spread of methylation and transcriptional silencing across a region of DNA (Zhang et al. 2008). Specifically, *S. pombe* exhibit important heterochromatin boundaries at three types of loci: the telomeric and pericentromeric regions of their chromosomes and at the silent mating type (MAT) locus (Kiely et al. 2011). The histone methyltransferase, Clr4, is initially recruited to sites targeted for silencing via sequence-specific DNA binding proteins or non-coding RNAs (Wang et al. 2016). The Clr4 methyltransferase methylates the lysine residue of the histone causing specific heterochromatin proteins to be recruited to this site. Heterochromatin protein 1 (HP1), termed Swi6 in *S. pombe,* interacts with H3K9me methylation marks to stabilize the localization of Clr4, which in turn, allows for the propagation of heterochromatin in a sequence-independent manner (Zhang et al. 2008). The Swi6 protein binds to the methylated H3 histone tails at lysine-9 residues and has been shown to be required for the formation of heterochromatin due to its ability to recruit the histone methyltransferase Clr4 (Nonaka et al. 2002; Halder et al. 2011). The HP1 family protein Swi6 interacts with H3K9me and induces the spread of heterochromatin in a dosage-dependent manner (Martin and Grewal 2006). This means that the spread of heterochromatin across a region of the genome depends of the concentration of Swi6 interacting with H3K9me. The spread of heterochromatin past specific boundaries and into gene coding regions is problematic in organisms from *S. pombe* to humans and can lead to the silencing of genes essential to cell growth or to tumor suppression, respectively (Garcia et al. 2015; Grewal and Songtao 2007).

Therefore, the spread of heterochromatin must be limited by specific factors so that it does not impact nearby transcriptionally active regions. Specifically, the inverted repeat (IR) elements of the MAT locus exhibits two factors enriched at the heterochromatin-euchromatin boundary, Epe1 and TFIIIC (Mizuguchi, Barrowman, and Grewal 2016).

Epe1 is a Jmjc domain containing protein that inhibits the spread of repressive histone methylation. Epe1 is recruited to heterochromatin by Swi6 in a boundary-independent manner in *S. pombe* and a similar function in mammals is proposed due to the highly-conserved nature of other HP1 family proteins (Figure 1; Lomberk et al. 2006). Epe1 has been shown to antagonize the spread of repressive histone methylation (Braun et al. 2010), yet is suggested to act in a way that constantly adjusts the strength of the heterochromatic state. On the other hand, Swi6 has been shown to promote the spread of repressive histone methylation (Zofall and Grewal 2006). This system maintains the heterochromatic state because Epe1 associates with Swi6 across the heterochromatin region, however is polyubiquitinated by a ubiquitin ligase and degraded, leaving Epe1 enriched at the boundaries (Braun et al. 2010). The preferential degradation of polyubiquitinated Epe1 in the middle of heterochromatic regions is not well understood, however, Epe1 remains enriched near heterochromatin boundaries and prevents the spread of silencing. In addition, phosphorylation of Swi6

within heterochromatic regions prevents an interaction with Epe1, allowing for association only near boundaries. While the functional Epe1 protein can be found throughout an entire heterochromatic region, the concentration of Epe1 at boundaries has been shown to contribute to effective heterochromatin boundary function (Wang et al. 2013).

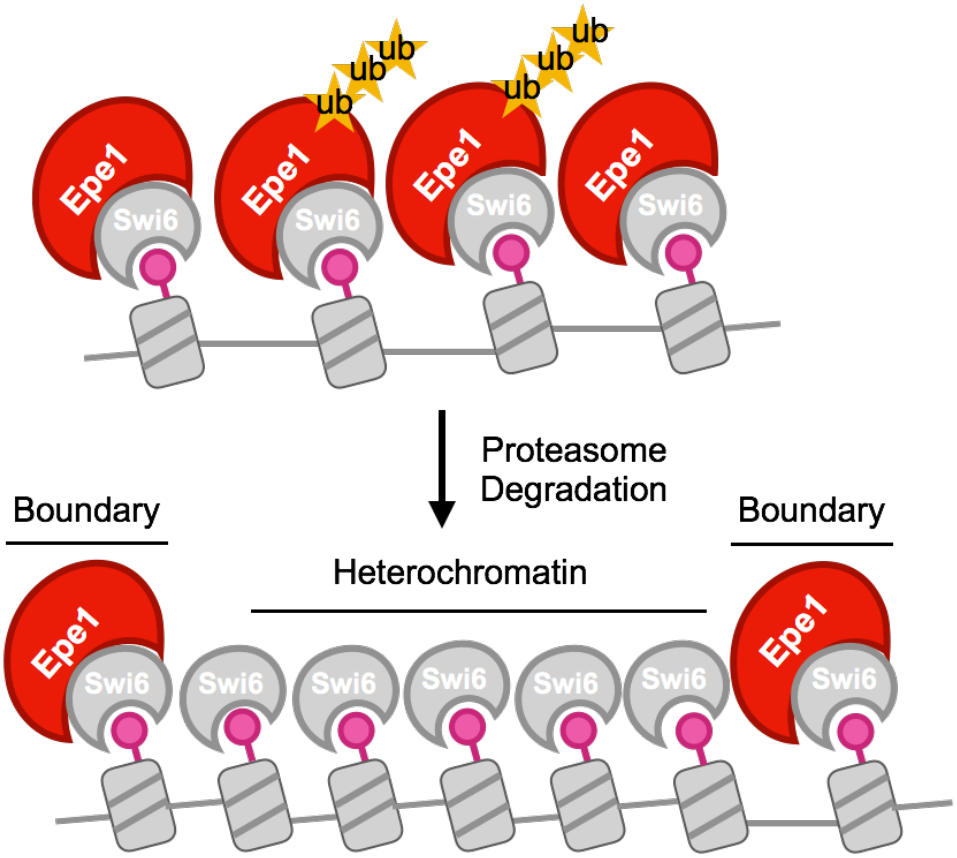

Figure 1. The Clr4 histone methyltransferase adds repressive histone methylation marks (pink lollipops) to H3 histone proteins within a heterochromatic region. These H3K9 methylation marks are recognized by the HP1 protein, Swi6 (grey). Epe1 (red) protein binds Swi6 within the heterochromatic region. Within the heterochromatic region, Epe1 is polyubiquitinated (yellow stars) which is recognized and degraded by the proteasome. This leaves Epe1 enriched at the heterochromatin boundary. (Diagram adopted from Braun et al. 2010)

The other factor that prevents the spread of heterochromatin into transcriptionally active areas of the genome is TFIIIC. TFIIIC is a transcription factor that can recruit the RNA polymerase III complex, which is responsible for transcription of specific classes of genes, including transfer RNAs (tRNAs). TFIIIC binds to DNA elements, termed *B-boxes*, in an RNA polymerase III-independent manner (Figure 2; Noma, Cam, Maraia, and Grewal, 2006). *B-box* sequences are found within the tRNA clusters and the inverted repeat elements of the mating type locus in *S. pombe,* both of which act as boundary elements (Kirkland et al. 2013; Noma et al. 2001; Partridge et al. 2000). Additionally, TFIIIC interacts with boundary sequences and together have been found to

localize to the nuclear periphery, possibly suggesting the use of tethering DNA to the nuclear envelope as a physical barrier between regions of transcriptional activity and silencing (Hiraga et al. 2012).

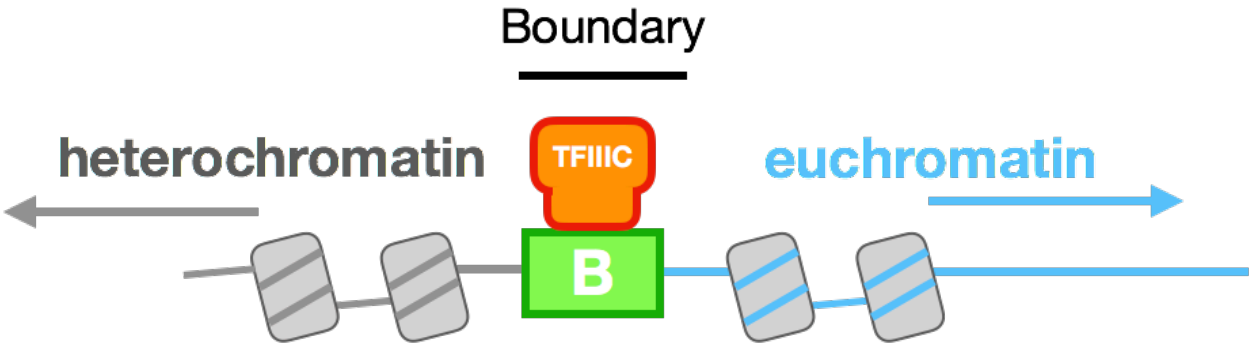

Figure 2. DNA sequence elements termed *B-boxes* (green box), recruit the TFIIIC transcription factor protein (orange) to the heterochromatin boundary, thus preventing the spread of repressive histone methylation into euchromatic regions of the genome (blue).

Together, both Epe1 and TFIIIC are essential to boundary function and act in parallel and redundant pathways that prevent the spread of deleterious heterochromatic silencing (Figure 3). Removal of either Epe1 or TFIIIC, individually, does not completely abolish boundary function and heterochromatin spreading is partially prevented by the factor that is properly performing its function. However, loss of both Epe1 and TFIIIC cause silencing to spread across a large region of the genome and can have extreme consequences including the silencing of nearby genes (Trewick et al. 2007; Noma, Cam, Maraia, and Grewal, 2006). Despite their redundant functions, the TFIIIC-dependent and Epe1-dependent pathways of boundary function have different mechanisms of activity to prevent the spread of repressive histone methylation (Garcia et al. 2015).

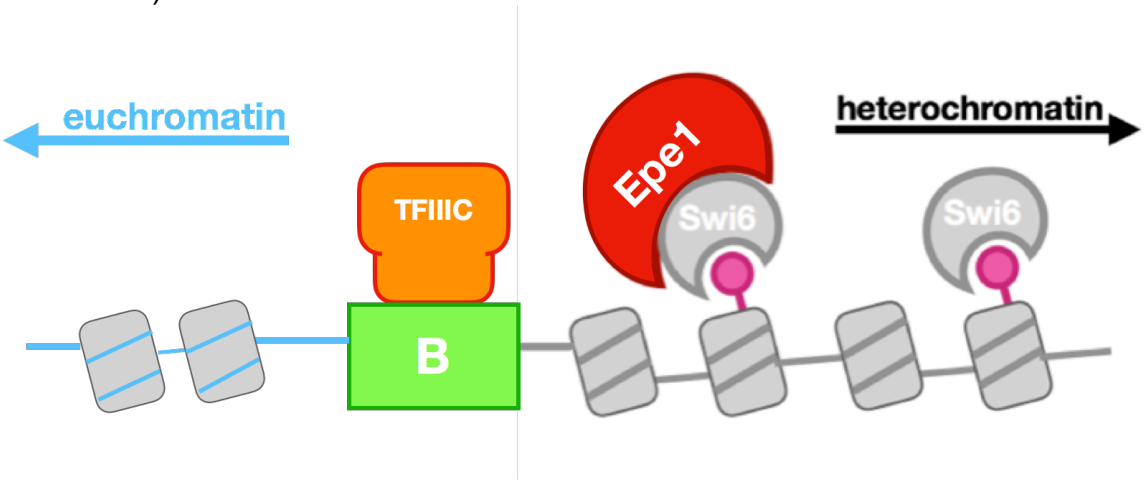

Figure 3. Epe1 and TFIIIC act in parallel and redundant pathways to prevent heterochromatin silencing. *B-box* DNA elements (green box) recruit TFIIIC (orange) to the boundary, while Epe1 (red) is preferentially enriched at the boundary and recruited

to heterochromatin by Swi6 (grey). These pathways act together to prevent the spread of repressive histone methylation into euchromatic regions.

Although an Epe1-dependent and TFIIIC-dependent pathway of heterochromatin boundary function has been discovered, the mechanisms by which they act and the other proteins involved in the pathways are relatively unknown. To elucidate these proteins and a potential mechanism for TFIIIC-dependent boundary function, a reporter construct used by Garcia et al. 2015 for boundary function was employed (Figure 4). This reporter is constructed with a Gal4 binding site, the *upstream activating sequence* (*UAS*) in between two reporter genes, *ura4+* and *ade6+*. Upstream of the *UAS* is a DNA insertion site where DNA elements can be tested for boundary function. In addition, strains were developed with the Gal4 protein fused with the Clr4 methyltransferase lacking its chromodomain, allowing for the targeting of the methyltransferase to the reporter construct via the interaction between the Gal4 DNA-binding domain and *UAS*.

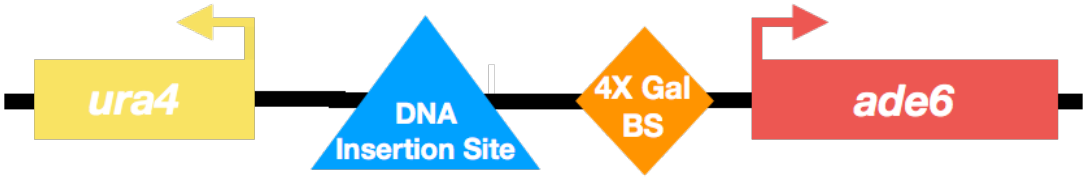

Figure 4. Schematic diagram of the reporter construct to assess the efficacy of heterochromatin boundary elements. The 4x Gal BS (orange diamond) recruits a GAL protein tethered Clr4 methyltransferase that induces the spread of heterochromatin. The DNA insertion site (blue triangle) allows for the insertion of DNA elements to test their ability to prevent the spread of repressive histone methylation. The *ura4+* gene (yellow box) acts to read out whether the DNA element functions as a boundary element while the *ade6+* marker (red box) acts as a control to assess the spread of repressive histone methylation across this gene coding region. (Diagram adopted from Garcia et al. 2015)

This reporter strain allowed for investigation into whether the DNA element inserted into the reporter construct represented a functional boundary element. Specifically, sequences from the IR-L that corresponded to *B-box* elements could be inserted into the DNA insertion site and tested for conferring boundary function on the reporter gene (Figure 5). With the insertion of a *B-box* element, TFIIIC is recruited to this region and establishes a functional boundary, preventing the spread of repressive histone methylation across the *ura4+* gene and allowing for its transcriptional expression. In addition, functional *B-box* elements could be inserted with the gene for *epe1* deleted, allowing us to test for the effects of Epe1 on boundary function. The reporter genes in the construct, *ura4+* and *ade6+* result in observable phenotypic differences when they are transcriptionally active or silent and when these fission yeast reporter strain are plated on YS-5 Fluoroorotic Acid (5-FOA) or media lacking adenine. If the *S. pombe* strain is expressing *ura4+* due to proper boundary function, cells die when plated on YS-5FOA. *Ade6+* acts as a control for repressive histone methylation since there are no boundary elements to prevent the spread of repressive histone methylation, and reporter strains plated on low adenine media produce a red phenotype due to the silencing of the *ade6* gene.

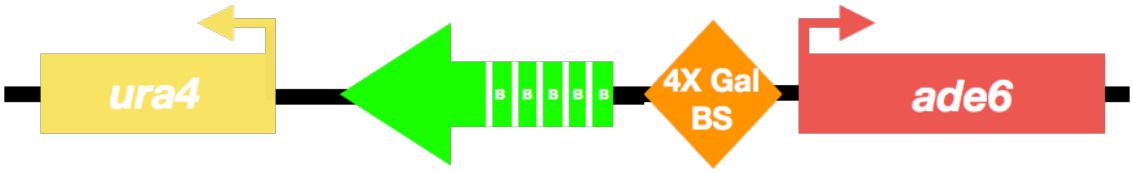

Figure 5. Schematic diagram of the reporter construct utilized in the forward genetic screen. *B-box* DNA sequence elements (green arrow) were inserted into the DNA insertion site of the reporter construct from the IR-L of the *S. pombe* MAT locus to assess the ability of TFIIIC to function as a boundary element. All other elements of the reporter are the same as described in Figure 4. (Diagram adopted from Garcia et al. 2015)

With this reporter strain, the genes specifically involved in the TFIIIC pathway can be elucidated by DNA mutagenesis and genetic screening to look for the lack of boundary function and resulting spread of repressive histone methylation. Chemical mutagenesis with ethyl methanosulfate (EMS) was employed in strains carrying the reporter strain and lacking Epe1 function to identify mutations that impaired TFIIIC boundary function. Mutants that displayed a phenotype that correlated with a lack of boundary function were sequenced and three mutants were determined to harbor mutations in the *sda1, cog5* and *dpb2 (cog5/dpb2),* and *byr3* genes. Mutations within the *sda1* gene have been shown to effect Epe1 function (Wang et al. 2015), while the gene product of *byr3*+ has been predicted to interact with Clr4 (Ryan et al. 2015). The *cog5* and *dpb2* mutations were isolated together from one mutant strain and their interactions and functions remain unknown.

To confirm the mutations disrupt the TFIIIC-dependent pathway of boundary function and rule out the possibility that the mutations identified in the genetic screen are not false positives, we designed CRISPR/Cas9 plasmids to target the wildtype gene and replace the region with the sequenced mutation. CRISPR/Cas9 gene editing is a technology taken from the adaptive immunity of bacteria designed to target and cleave a specific DNA sequence. The Cas9 protein is an endonuclease that uses a guide sequence RNA to recognize a sequence within the host DNA and induce site-specific double-stranded DNA breaks (Doudna and Charpentier 2014). By inserting a piece of DNA with homology to the region that was targeted by CRISPR/Cas9, the cell's endogenous repair mechanisms can be utilized to reintroduce the mutant sequence and strains can be observed for impaired TFIIIC-dependent boundary function (Figure 6). This will be performed in strains that have the *epe1* deletion and are wildtype for TFIIIC function. The CRISPR/Cas9 system will be used to introduce the prospective mutation back into the genome and impair boundary function. This, in turn, confirms that the mutations induced by mutagenesis act within the TFIIIC-dependent pathway of boundary function.

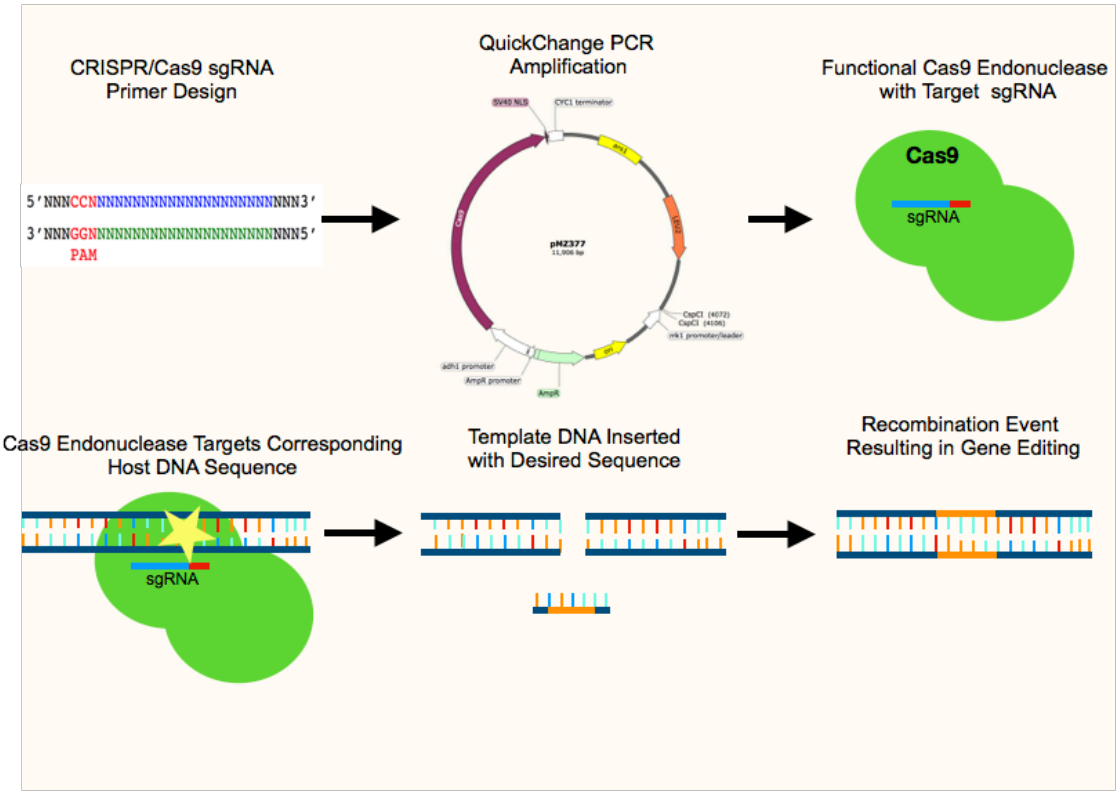

Figure 6. Flow chart of the CRISPR/Cas9 methodology for gene editing. sgRNA primers were designed utilizing sequencing results from the forward genetic screen performed by the Madhani lab and according to the protocol described by Rodríguez-López et al. 2017. sgRNA primers were inserted into the CRISPR/Cas9, pMZ377 plasmid via QuickChange PCR amplification. QuickChange was employed as an efficient method to engineer different plasmids with the respective sgRNA inserts for each target gene. The plasmid containing the sgRNA insert is then amplified and transformed into *S. pombe*, where the Cas9 protein is translated with the sgRNA sequence and expressed (green circles). The Cas9 protein targets the corresponding DNA sequence to the sgRNA sequence, inducing a double-stranded DNA break (yellow star). Template DNA (orange) of the desired sequence to be edited into the host genome can be added to the cell with flanking regions of homology (blue), allowing for a recombination event to occur with the desired sequence. The recombination event occurs at the specific site of the ds-DNA break due to the homology of the template strand with the specific region of DNA, allowing for site-specific gene editing.

Results:

Confirming Efficacy of the Boundary Reporter Strains.

To gain insight into the mechanisms of boundary function, the reporter construct described by Garcia et al. 2015 was employed using plate growth assays. Selective media was utilized to allow for the phenotypic read out of whether the reporter was transcriptionally active or silenced due to a functioning boundary or the spreading of repressive histone methylation across the reporter, respectively. The reporter construct works to read out the spread of repressive histone methylation by recruiting a recombinant and altered histone methyltransferase Clr4 fused with a GDB binding domain protein (GDB-Clr4-CD△). This is recruited to the reporter construct by a 4X *UAS* sequence, also referred to as the 4X *Gal* binding site (*4X GAL BS*), and allows for DNA boundary elements to be tested with the DNA insertion site. The spread of repressive histone methylation is measured by the repression of *ura4+* determined by the growth of *S. pombe* cells on YS-5FOA media, while growth on YS media serves as a control. Additionally, the *ade6+* reporter gene serves as a control for the spread of repressive histone methylation and can be read on low adenine media (Figure 1A).

The results discovered by Garcia et al. 2015 were retested to confirm that the phenotypes of the wild-type (WT) reporter strain, individual *b-box△* and *epe1△* mutant strains containing the reporter, and *epe1△*/ *b-box△* double mutant reporter strain were behaving according to the results described in the plate growth assays (Figure 1B). Due to the excessive growth of the *b-box△* single mutant on YS-5FOA media, genetic clones of this strain were plated and assessed for proper phenotypic growth on YS-5FOA and selected for representative growth. In addition, the lack of growth of the *epe1△*/ *b-box△* double mutant strain on YS-5FOA was also inconsistent with the results described by Garcia et al. 2015, therefore, genetic clones of the double mutant were also plated and assessed for the proper representative phenotypic growth on YS-5FOA media. Genetic clones of the *b-box△* single mutant and *epe1△*/ *b-box△* double mutant strains were selected for future plate growth assays and with the control strains functioning properly, we began to assess the specific candidate factors involved in the TFIIIC-dependent pathway of heterochromatin boundary function.

EMS Mutants Display Strong Growth On YS-5FOA Media.

To determine candidate factors involved in the TFIIIC-dependent pathway of heterochromatin boundary function, a forward genetic screen was performed by the Madhani laboratory utilizing the boundary reporter strain containing the wildtype *IR-L* with functional B-boxes (Figure 2A) and harboring an *epe1△*. Chemical mutagenesis was performed in the *epe1△* strain and then screened for resulting cells that exhibited a complete loss of boundary function on 5-FOA media. Three mutant strains identified as exhibiting lack of boundary function were sequenced using Sanger DNA Sequencing and analyzed for mutations that may be implicated in the TFIIIC-dependent pathway of heterochromatin boundary function. The analysis returned four candidate genes harbored in three mutant strains. This analysis identified mutations in the *sda1, byr3,* and *cog5,* and *dpb2* genes.

To confirm the mutagenesis results performed in the Madhani laboratory, the *S. pombe* strains harboring the *sda1, byr3,* and *cog5/dpb2* mutations were pinned against

the WT reporter strain, the *epe1*△ reporter strain, the *b-box*△ reporter strain, and the *epe1*△/ *b-box*△ double-mutant reporter strain (Figure 2B). This also served as a confirmation that the mutant strains were behaving correctly, that the assay to test for boundary function was valid, and the mutant phenotypes are reproducible. The WT reporter strain exhibits growth on the control, YS media however cannot grow on the YS-5FOA due to expression of *ura4+* as a result of a functioning boundary. The *epe1*△ reporter strain and the *b-box*△ reporter strain both exhibit growth on the control media, YS, and grow minimally on 5-FOA due to some loss of boundary function, however, the growth is minimal compared to the double mutant. The *epe1*△/ *b-box*△ double-mutant reporter strain exhibits similar growth on both YS and YS-5FOA due to a lack of boundary function and spreading of heterochromatin over the *ura4+* reporter gene.

Similarly, the three mutant phenotypes presumed to have mutations that affect the TFIIIC-depending pathway of heterochromatin boundary function and harbor the *epe1*△ mutation, exhibit a phenotype like that of the double mutant due to complete loss of boundary function. The mutant phenotypes were verified on YS and YS-5FOA consistently, showing proper phenotypic growth on both media. However, the EMM - adenine plate phenotypes described by Garcia et al. 2015 were inconsistent with previously published results, and the growth of the reporter and mutant strains on this media was variable. The *ade6+* marker contained on the reporter construct acts to read out the spread of repressive histone methylation from the Clr4-recruitment site and will cause cells to turn red as the presence or lack of boundary elements does not affect the ability of heterochromatin to spread to this portion of the reporter. Therefore, the cells containing the reporter strain plated on low-adenine plates should exhibit a red phenotype due to the inability to synthesize adenine. Due to the varying growth of the reporter strains on the EMM – adenine selective media, the plating assay was also attempted with synthetic complete (SC) media lacking adenine, however, the results, again, were inconsistent across the reporter strains and growth of the reporter and mutant strains was stunted or non-existent.

Employing a CRISPR/Cas9 System to Confirm Mutants Implicated in the TFIIIC-Dependent Pathway of Boundary Function.

To test if the mutations in the genes discovered through the genetic screen impair the TFIIIC-dependent pathway of boundary function, we decided to employ a CRISPR/Cas9 system to mutate the wildtype sequence of these genes and replace them with the single point mutation that rendered boundary function inactive. The Addgene CRISPR/Cas9 plasmid employed by Rodríguez-López et al. 2017, pMZ377, was selected for the experiments due to the *Leu2* marker contained on the plasmid (Figure 3A). This marker does not interfere with other markers utilized in the boundary function assay and the reporter strains. By utilizing a sgRNA sequence targeted to the wildtype sequence, and template DNA from the mutant strains the mutation can be inserted into the correct region of the host DNA. The same logic can be applied reciprocally, with the mutant gene targeted in the mutant strains, and restoring boundary function by introducing a WT sequence. The CRISPR/Cas9 sgRNA sequences were selected based on their proximity to the mutations identified by sequencing results from the mutagenesis screen and to a PAM sequence, essential for Cas9 function.

A QuickChange PCR protocol was utilized to amplify sgRNA primer sequences corresponding to the WT gene target into the pMZ377 plasmid. Initially, only the *cog5* and *sda1* sgRNA primers were used to confirm that the primers were designed correctly and could be inserted into the plasmid. The PCR reactions were optimized using 2% DMSO to stabilize the large PCR product. With successful QuickChange PCR reaction of the sgRNA into pMZ377, the insertion of the sgRNA results in the loss of a CspCI cutsite, resulting in a plasmid lacking this cut site after ligation and transformation. The plasmid was checked by restriction enzyme digest with CspCI and run by gel electrophoresis to determine the correct length of the plasmid.

Successful Transformation of pMZ377 Containing CRISPR/Cas9 sgRNA Inserts Can Be Visualized by Restriction Enzyme Digest.

The purified CRISPR/Cas9 plasmids were restriction enzyme digested with CspCI to confirm the insertion of the sgRNA insert into the correct location of the plasmid (Figure 4). Purified samples of pMZ377 were cut with CspCI to visualize cut versus uncut plasmid (Figure 4A), similar to the results expected from successful sgRNA insertion into the plasmid. The imaging results from the restriction enzyme digest of purified pMZ377 allow us to differentiate between the uncut from the cut plasmids while additionally, utilizing the CspCI digest to check for the correct length of the plasmid and remove false positives before samples were sent for sequencing.

The pMZ377 plasmids that were confirmed by gel electrophoresis after QuickChange sgRNA PCR to be the expected length were transformed in to *Escherichia coli* (*E. coli*) and selectively grown on ampicillin-containing media to select for bacteria that contained the plasmid. Four individual drug-resistant colonies were selected from each transformation containing the respective sgRNA insert and plasmids were isolated from these cells. The isolated plasmids were restriction enzyme digested with CspCI and compared against purified pMZ377 CspCI restriction enzyme digestion to confirm sgRNA insertion and to eliminate false positive vectors that did not contain the complete pMZ377 yet conferred drug resistance (Figure 4B). The false positives are likely abbreviated forms of the CRISPR/Cas9 plasmid containing the bacterial drug resistant marker, conforming bacterial resistance to the *E. coli* colonies and allowing them to grow on the selective media. With the confirmation of the correct length plasmid from gel electrophoresis of the PCR products and restriction enzyme digest products, plasmids were prepared and sent for sequencing.

The M13-Forward Sequencing Primer Binds Multiple Sites on the pMZ377 Plasmid.

The CRISPR/Cas9 plasmids that were identified as containing their respective sgRNA sequences from restriction enzyme digest with CspCI were sent for sequencing with the M13-forward primer, according to the protocol described by Rodríguez-Lopez et al. 2017. These sequencing results were returned with inconclusive reads containing multiple peaks (Figure 5A). To test if the pMZ377 plasmid contained multiple binding sites for the M13-forward sequencing primer, the pure pMZ377 *E. coli* colony was streaked for singles, isolated, and sent for sequencing along with the clones that were determined to be of the correct length from CspCI restriction enzyme digestion (Figure 4). The sequencing results for the purified plasmid and the plasmids containing the

sgRNA sequences were returned with inconclusive read outs containing multiple peaks (Figure 5A). This suggested that the primer was binding to multiple sites on the plasmid, however, a ligation free protocol from Rodríguez-López et al. 2017 was utilized to create the *sda1* sgRNA CRISPR/Cas9 plasmids. These plasmids were transformed, plated on selective media, and isolated, then were digested with CspCI to confirm the sgRNA insertion and expected plasmid length. Again, sequencing was performed with the M13-forward primer and the results were returned with multiple peaks and deemed inconclusive (Figure 5A).

This led us to attempt sequencing the plasmids utilizing a different primer. Upon analysis with Quintarabio Primer Binding Database, it was determined that the M13-forward primer binds multiple sites on the pMZ377 plasmid, and that the QB2396 primer had only one binding site near the sgRNA insertion site on the pMZ377 plasmid. The pMZ377 plasmids with sgRNA inserts that were prepared with the ligation protocol were prepared and sent for sequencing with the QB2396 primer. The Rodríguez-López et al. 2017 paper suggests M13 Forward as a suitable primer for sequencing of pMZ377, however, sequencing results suggest that this primer binds multiple sites on the plasmid and that the QB2396 primer is capable of detecting the sgRNA sequence at the plasmid insertion site.

The *sda1* sgRNA samples from the initial sgRNA QuickChange PCR with pMZ377 (Figure 4B) were resent for sequencing analysis and were returned with results that matched the expected product for the reaction (Figure 5B). The rest of the CRISPR/Cas9 sgRNA plasmids identified by restriction enzyme digest were also sent for sequencing after successful return of *sda1* results. These sgRNA CRISPR/Cas9 plasmids were analyzed for the correct insertion of the sgRNA sequence and were confirmed to contain the correct sequence. Therefore, we can reason that the M13 forward sequencing primer was binding to multiple sites on the pMZ377 plasmid. Moving forward, the *sda1* CRISPR/Cas9 sgRNA plasmid will be transformed into the WT reporter strain and *epe1*△ reporter strain to target the WT *sda1* gene and edit the gene to contain the mutant sequence discovered from the mutagenesis. Template DNA containing the mutant *sda1* sequence will be inserted into this specific site to confirm the results of the Madhani genetic screen and, ultimately, elucidate if this factor and the other factors involved are implicated in the TFIIIC-dependent mechanism for boundary function.

Discussion:

The Epe1- and TFIIIC-mediated pathways of heterochromatin boundary maintenance act in parallel and redundant pathways to prevent the unchecked spread of heterochromatin across gene coding regions of DNA in *S. pombe*. Although these two pathways are well described and the consequences of their failure can be examined utilizing the reporter described by Garcia et al. 2015, intermediate proteins that affect the proper function of the Epe1- and TFIIIC-mediated pathways have not been illuminated. We purposefully examined Epe1 knockout strains in a genetic screen using EMS to determine candidate genes involved in the TFIIIC-dependent pathway of heterochromatin boundary function. Mutants that lost the ability to maintain boundary function in this genetic screen were sequenced and analyzed and four genes in three separate strains were identified. These mutations were single base pair changes that resulted in lack of TFIIIC-dependent boundary function, and were identified in the *sda1, byr3,* and *dpb2,* and *cog5* genes. The function of these genes as they relate to boundary function in *S. pombe* are not well understood, however, some other functions of these proteins have been described. Wang et al. 2015 suggests that Sda1 interacts with Epe1 and promotes its function. The findings from this mutagenesis study implies an alternative role for Sda1 in the TFIIIC-dependent pathway of heterochromatin formation. The role of Byr3 has been predicted by Ryan et al. 2015 to interact with the Clr4 histone methyltransferase, which is a key component of heterochromatin formation in *S. pombe* and utilized by the reporter construct in this study to induce heterochromatin spread. Therefore, a novel function for Byr3 in heterochromatin boundary function may occur based on its association and interaction with Clr4. The literature describing the *sda1*+ and *byr3*+ genes suggest a potential role in heterochromatin formation and maintenance, while the *dpb2* and *cog5* mutations have not been described and were investigated individually in this research.

To examine and confirm the results from the genetic screen that *sda1*+*, byr3*+*, dpb2*+*,* and *cog5*+ genes are involved in the TFIIIC-dependent pathway of heterochromatin boundary function, we employed a CRISPR/Cas9 gene editing tool. The CRISPR sgRNAs were engineered to target the WT gene identified in mutagenesis and through homologous recombination, template DNA containing the mutant base pair change would be inserted at the correct location. This same strategy can be applied in reverse to confirm the results and specificity of the CRISPR/Cas9 gene editing tool. However, the methodology has not been employed due to complications with the sgRNA insert, CRIPSR/Cas9 plasmid, sequencing results. The QuickChange protocol was run according to procedures outlined in Rodríguez-López et al. 2017 and checked by gel electrophoresis and restriction enzyme digest for correct length of the plasmid. After confirmation of the expected length of the plasmid, samples were prepared and sent for sequencing with the M13 forward primer. The sequencing samples were consistently returned with the result of inconclusive*.* A sample was sent of the unaltered plasmid, pMZ377, and the results were also inconclusive*,* suggestive that the M13 forward primer has multiple binding sites on CRISPR/Cas9 plasmid, pMZ377.

Although these inconclusive sequencing results have halted the process of transforming and implementing the CRISPR/Cas9 tool to edit the genome of cells with WT function and determine if these genes are involved in TFIIIC-mediated heterochromatin boundary function, we have found the potential source of the issue.

The CRISPR/Cas9 plasmids will be prepared, again and sent for sequencing using the Quintarabio QB2936 sequencing primer, which is a longer, more specific primer for the sgRNA insertion site that is less likely to bind to alternative sites. Clear sequencing results will allow for the experiment to progress and for plasmids to be transformed in *S. pombe,* allowing us to implement the methodology described above and confirm if *sda1+, byr3+, cog5+,* and *dpb2+* act within the TFIIIC-mediated pathway of heterochromatin boundary function.

Confirming the *sda1+, byr3+, cog5+,* and *dpb2+* genes as functioning in the TFIIIC-mediated pathway of heterochromatin boundary maintenance will allow more detailed and focused studies on their exact function and potential mechanisms within boundary function. It will be especially interesting to investigate the idea that *sda1+* acts within both pathways and could be a crucial intermediate to both the TFIIIC- and Epe1-mediated pathways of heterochromatin boundary maintenance.

Acknowledgements:

pMZ377 was a gift from Mikel Zaratiegui. I would like to thank Colorado College and the student-faculty collaborative research program and trustee, Colburn S. Wilbur for providing funding for this research. A special thanks to Delaine Winkelblech for technical support and Dr. Darrell J. Killian for his assistance. I would like to express my sincere gratitude to my advisor Dr. Jennifer F. Garcia for the continuous support of my studies and related research, for her patience, motivation, and immense knowledge. I would also like to thank Dean Edmonds for his unwavering support in my academic success.

Table 1. Strains used in this research

Strain	Genotype
PM 0004	*h- ade6-M210. leu1-32, ura4-D18, smt0*
PM 1572	*h- can1::ura4+-tRNA-4xGal UAS-ade6+, clr4△::hphMX-Gal4DBD-clr4-CD△, ade6- M210, leu1-32, ura4-D18*
PM 1860	*h- can1::ura4+-tRNA-4xGal UAS-ade6+, clr4△::hphMX-Gal4DBD-clr4-CD△, ade6- M210, leu1-32, ura4-D18; epe1△*
PM 1779	*h- can1::ura4+-IR-L MT1 (-327 bp)-4xGal UAS-ade6+, clr4△::hphMX-Gal4DBD-clr4-CD△, ade6- M210, leu1-32, ura4-D18, smt0*
PM 1780	h- can1::ura4+-IR-L MT1 (-327 bp)-4xGal UAS-ade6+, clr4△::hphMX-Gal4DBD-clr4-CD△, ade6- M210, leu1-32, ura4-D18, smt0
PM 1781	*h- can1::ura4+-IR-L MT1 (-327 bp)-4xGal UAS-ade6+, clr4△::hphMX-Gal4DBD-clr4-CD△, ade6- M210, leu1-32, ura4-D18, smt0*
PM 1782	*h- can1::ura4+-IR-L MT1 (-327 bp)-4xGal UAS-ade6+, clr4△::hphMX-Gal4DBD-clr4-CD△, ade6- M210, leu1-32, ura4-D18, smt0*
PM 1783	*h- can1::ura4+-IR-L MT1 (-327 bp)-4xGal UAS-ade6+, clr4△::hphMX-Gal4DBD-clr4-CD△, ade6- M210, leu1-32, ura4-D18, smt0*
PM 1784	*h- can1::ura4+-IR-L MT1 (-327 bp)-4xGal UAS-ade6+, clr4△::hphMX-Gal4DBD-clr4-CD△, ade6- M210, leu1-32, ura4-D18, smt0*
PM 1785	*h- can1::ura4+-IR-L MT1 (-327 bp)-4xGal UAS-ade6+, clr4△::hphMX-Gal4DBD-clr4-CD△, ade6- M210, leu1-32, ura4-D18, smt0*
PM 1786	*h- can1::ura4+-IR-L MT1 (-327 bp)-4xGal UAS-ade6+, clr4△::hphMX-Gal4DBD-clr4-CD△, ade6- M210, leu1-32, ura4-D18, smt0*
PM 1787	*h- can1::ura4+-IR-L MT1 (-327 bp)-4xGal UAS-ade6+, clr4△::hphMX-Gal4DBD-clr4-CD△, ade6- M210, leu1-32, ura4-D18, smt0*
PM 1809	*h- can1::ura4+-IR-L MT1 (-327 bp)-4xGal UAS-ade6+, clr4△::hphMX-Gal4DBD-clr4-CD△, epe1△::kanMX, ade6- M210, leu1-32, ura4-D18, smt0*
PM 1810	*h- can1::ura4+-IR-L MT1 (-327 bp)-4xGal UAS-ade6+, clr4△::hphMX-Gal4DBD-clr4-CD△, epe1△::kanMX, ade6- M210, leu1-32, ura4-D18, smt0*
PM 1811	*h- can1::ura4+-IR-L MT1 (-327 bp)-4xGal UAS-ade6+, clr4△::hphMX-Gal4DBD-clr4-CD△, epe1△::kanMX, ade6- M210, leu1-32, ura4-D18, smt0*
PM 1812	*h- can1::ura4+-IR-L MT1 (-327 bp)-4xGal UAS-ade6+, clr4△::hphMX-Gal4DBD-clr4-CD△, epe1△::kanMX, ade6- M210, leu1-32, ura4-D18, smt0*
PM 1813	*h- can1::ura4+-IR-L MT1 (-327 bp)-4xGal UAS-ade6+, clr4△::hphMX-Gal4DBD-clr4-CD△, epe1△::kanMX, ade6- M210, leu1-32, ura4-D18, smt0*
PM 1814	*h- can1::ura4+-IR-L MT1 (-327 bp)-4xGal UAS-ade6+, clr4△::hphMX-Gal4DBD-clr4-CD△, epe1△::kanMX, ade6- M210, leu1-32, ura4-D18, smt0*
PM 1815	*h- can1::ura4+-IR-L MT1 (-327 bp)-4xGal UAS-ade6+, clr4△::hphMX-Gal4DBD-clr4-CD△, epe1△::kanMX, ade6- M210, leu1-32, ura4-D18, smt0*
PM 1816	*h- can1::ura4+-IR-L MT1 (-327 bp)-4xGal UAS-ade6+, clr4△::hphMX-Gal4DBD-clr4-CD△, epe1△::kanMX, ade6- M210, leu1-32, ura4-D18, smt0*
PM 1817	*h- can1::ura4+-IR-L MT1 (-327 bp)-4xGal UAS-ade6+, clr4△::hphMX-Gal4DBD-clr4-CD△, epe1△::kanMX, ade6- M210, leu1-32, ura4-D18, smt0*
PM 2101	*h- can1::ura4+-IR-L MT1 (-327 bp)-4xGal UAS-ade6+, clr4△::hphMX-Gal4DBD-clr4-CD△, ade6- M210, leu1-32, ura4-D18, smt0, sdα1 mt*
PM 2102	*h- can1::ura4+-IR-L MT1 (-327 bp)-4xGal UAS-ade6+, clr4△::hphMX-Gal4DBD-clr4-CD△, ade6- M210, leu1-32, ura4-D18, smt0, byr3 mt*

PM 2104	*h- can1::ura4+-IR-L MT1 (-327 bp)-4xGal UAS-ade6+, clr4△::hphMX-Gal4DBD-clr4-CD△, ade6-M210, leu1-32, ura4-D18, smt0, cog5/dpb2 mt*

Table 2. Primers used in this research

Target:	Primer Name:	Sequence:
*sda1*sgRNA ligation free PCR #1 forward primer	CC37_sgFw_SDA1_1	5'-GGC AGA TTT CAT GAT GTT TAG TTT TAG AGC TAG AAA TAG CAA GTT AAA ATA A-3'
sda1 sgRNA ligation free PCR #1 reverse primer	CC38_sgRv_SDA1_1	5'-TAA ACA TCA TGA AAT CTG CCT TCT TCG GTA CAG GTT ATG TTT TTT GGC AAC A-3'
*sda1*sgRNA ligation free PCR #2 forward primer	CC35_sgFw_SDA1_2	5'-TAA ACA TCA TGA AAT CTG CCT TCT TCG GTA CAG GTT ATG TTT TTT GGC AAC A-3'
sda1 sgRNA ligation free PCR #2 reverse primer	CC36_sgRv_SDA1_2	5'-CAC TAT CAT CAA ACC CCA AAT TCT TCG GTA CAG GTT ATG TTT TTT GGC AAC A-3'
cog5 sgRNA forward PCR primer	BR1-COG5-gRNA-F	5'- AAA ACT AGA ACA ATT GAT GTG TTT TAG AGC TAG AAA TAG C-3'
cog5 sgRNA reverse PCR primer	BR2-COG5-gRNA-R	5'-ACA TCA ATT GTT CTA GTT TTT TCT TCG GTA CAG GTT ATG-3'
dpb2 sgRNA forward PCR primer	BR3-DPB2-gRNA-F	5'-TAT GGGT AGG CAT TTC AGC TAG TTT TAG AGC TAG AAA TAG C-3'
dpb2 sgRNA reverse PCR primer	BR4-DPB2-gRNA-R	5'-TAG CTG AAA TGC CTA CCA TAT TCT TCG GTA CAG GTT ATG-3'
byr3 sgRNA forward PCR primer	BR5-BYR3-gRNA-F	5'-TCA CAC GCT CCT ATT TAT TAG TTT TAG AGC TAG AAA TAG C-3'
byr3 sgRNA reverse PCR primer	BR6-BYR3-gRNA-R	5'- TAA TAA ATA GGA GCG TGT GAT TCT TCG GTA CAG GTT ATG-3'
sda1 sgRNA forward PCR primer	BR7-SDA1-gRNA-F	5'-GGC AGA TTT CAT GAT GTT TAG TTT TAG AGC TAG AAA TAG C-3'
sda1 sgRNA reverse PCR primer	BR8-SDA1-gRNA-R	5'- TAA ACA TCA TGA AAT CTG CCT TCT TCG GTA CAG GTT ATG-3'
M13 Forward	M13 F	5'-GTA AAA CGA CGG CCA GT-3'
QB2396 Sequencing Primer	QB2396	5'- GCGATCGGTGCGGGCCTCTT -3'

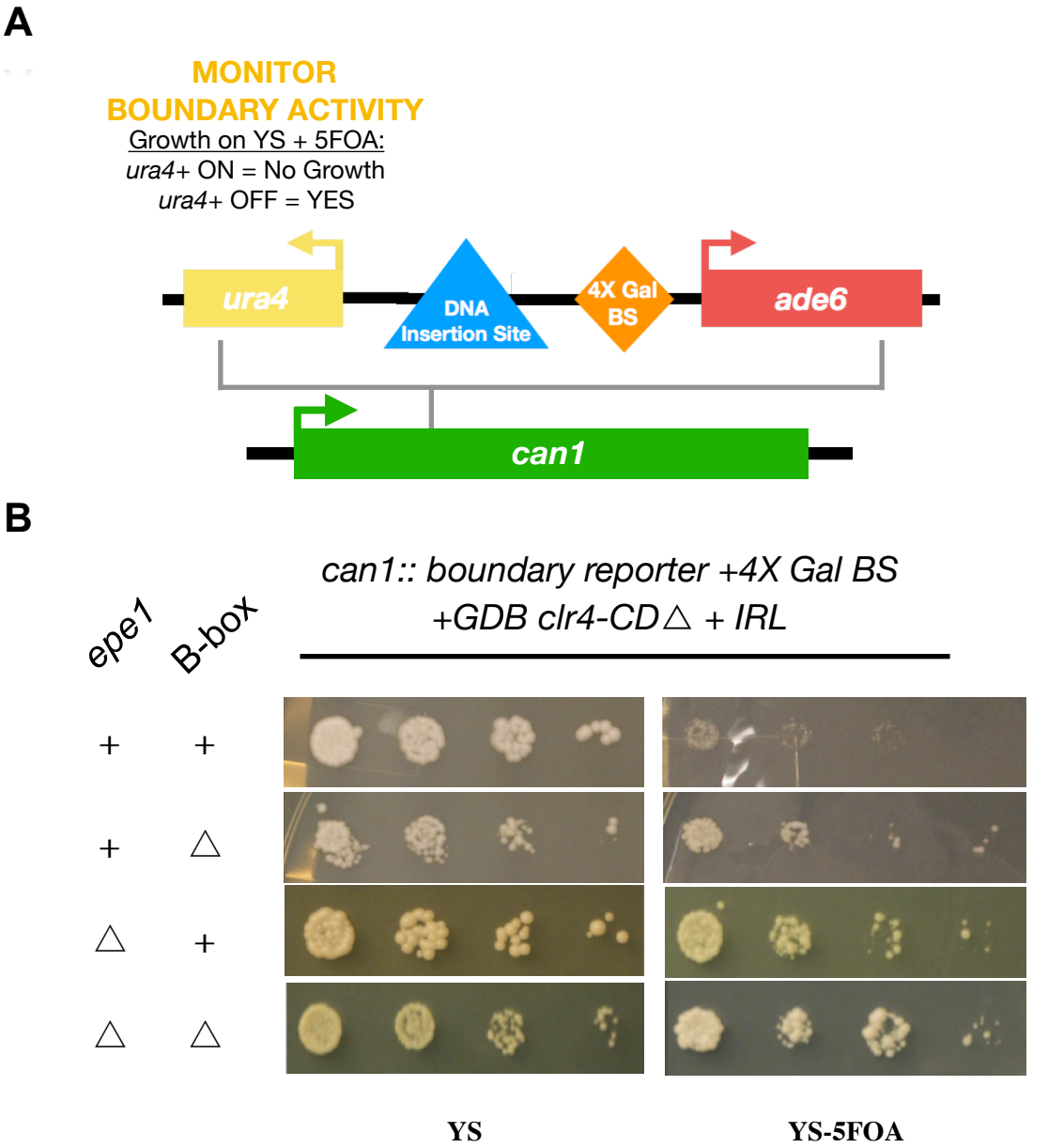

Figure 1. Confirming the Reporter Strain Activity and Phenotypes of Genetic Clones. The IR-L element promotes boundary activity in the reporter construct. (**A**) Schematic illustrating the boundary reporter inserted into the *can1+* locus. Blue triangle indicates a DNA insertion site, where boundary elements can be inserted and tested for efficacy. Orange diamond indicates the 4x Gal binding sites that are incorporated into the reporter construct to recruit GDB-Clr4-CD△, to promote heterochromatin silencing. (**B**) Growth assays performed on YS, rich media (control) and YS-5FOA, rich media combined with the drug 5FOA (Strain PM04 (WT); Strain PM 1784 (*b-box*△); Strain 1860 (*epe1*△); and strain 1813 (*epe1*△*/b-box*△)). Strains were grown to OD_{600} = 0.6, then back-diluted to OD_{600} = 0.4. Fivefold serial dilutions were pinned onto the respective media and grown at 30º C for 48 hours and were photographed. Representative photographs of genetic clones were combined to demonstrate expected results.

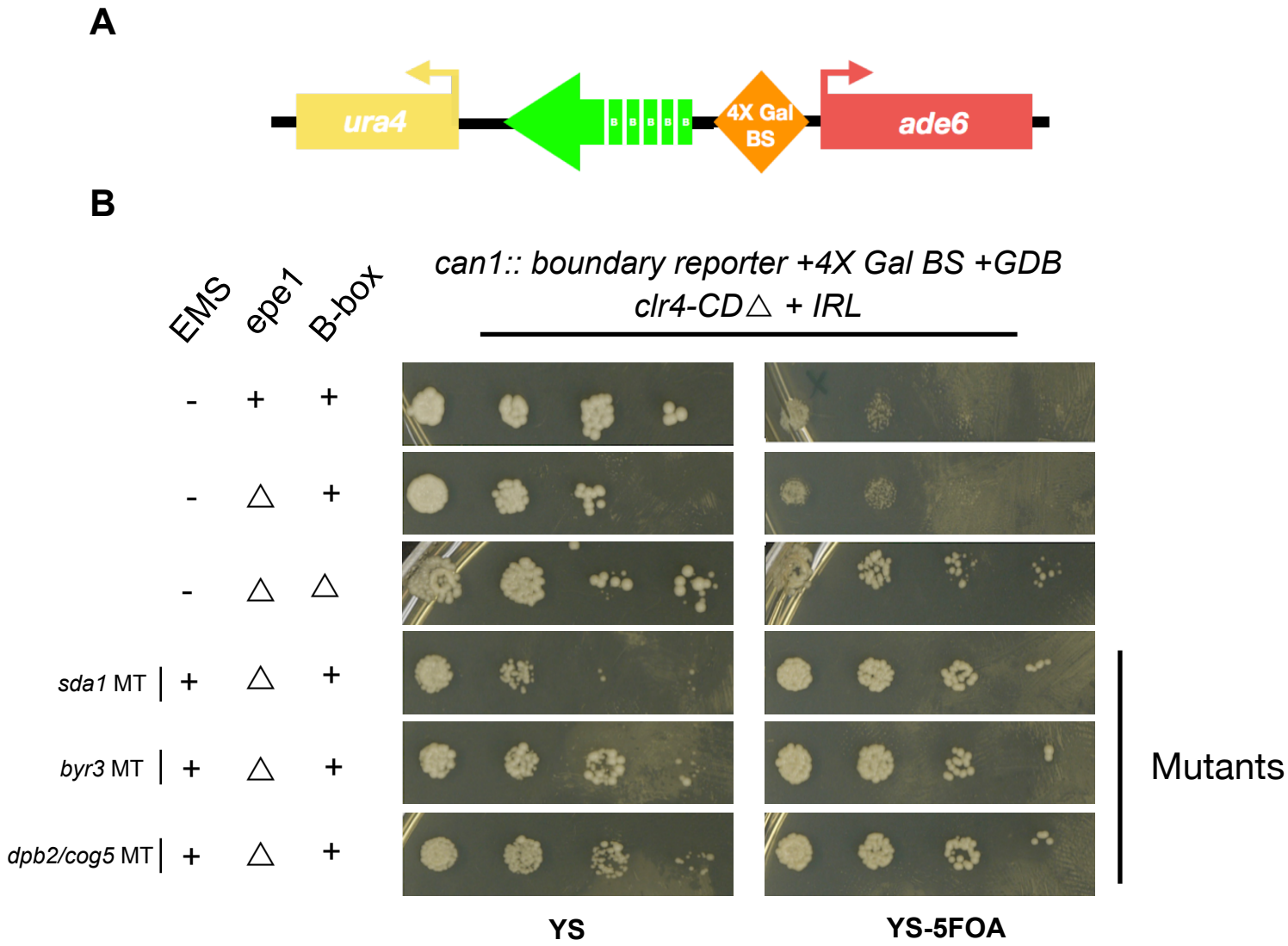

Figure 2. Confirming the Phenotypes of the Mutants isolated within the TFIIIC pathway of boundary activity. (**A**) Schematic of the reporter construct utilized in the mutagenesis screen for factors involved in the TFIIIC-dependent pathway of heterochromatin silencing. The *S. pombe IR-L* (green arrow) was inserted into the DNA insertion site with functional *B-box* elements (white boxes) that recruit functional TFIIIC protein to establish the heterochromatin boundary and was utilized to screen for loss of boundary function due to mutagenesis. (**B**) Mutations identified from a genetic screen implicated in the TFIIIC pathway of boundary activity were pinned against the strains confirmed in Figure 1B, utilizing the same protocol. Additionally, strains were pinned on EMM –ade, minimal media lacking adenine to read out the presence of the reporter in the *can1+* locus. The mutants were discovered in a forward genetic screen testing for impairment in the TFIIIC pathway of boundary function and mimic the phenotype of the *epe1△/b-box△* double mutant.

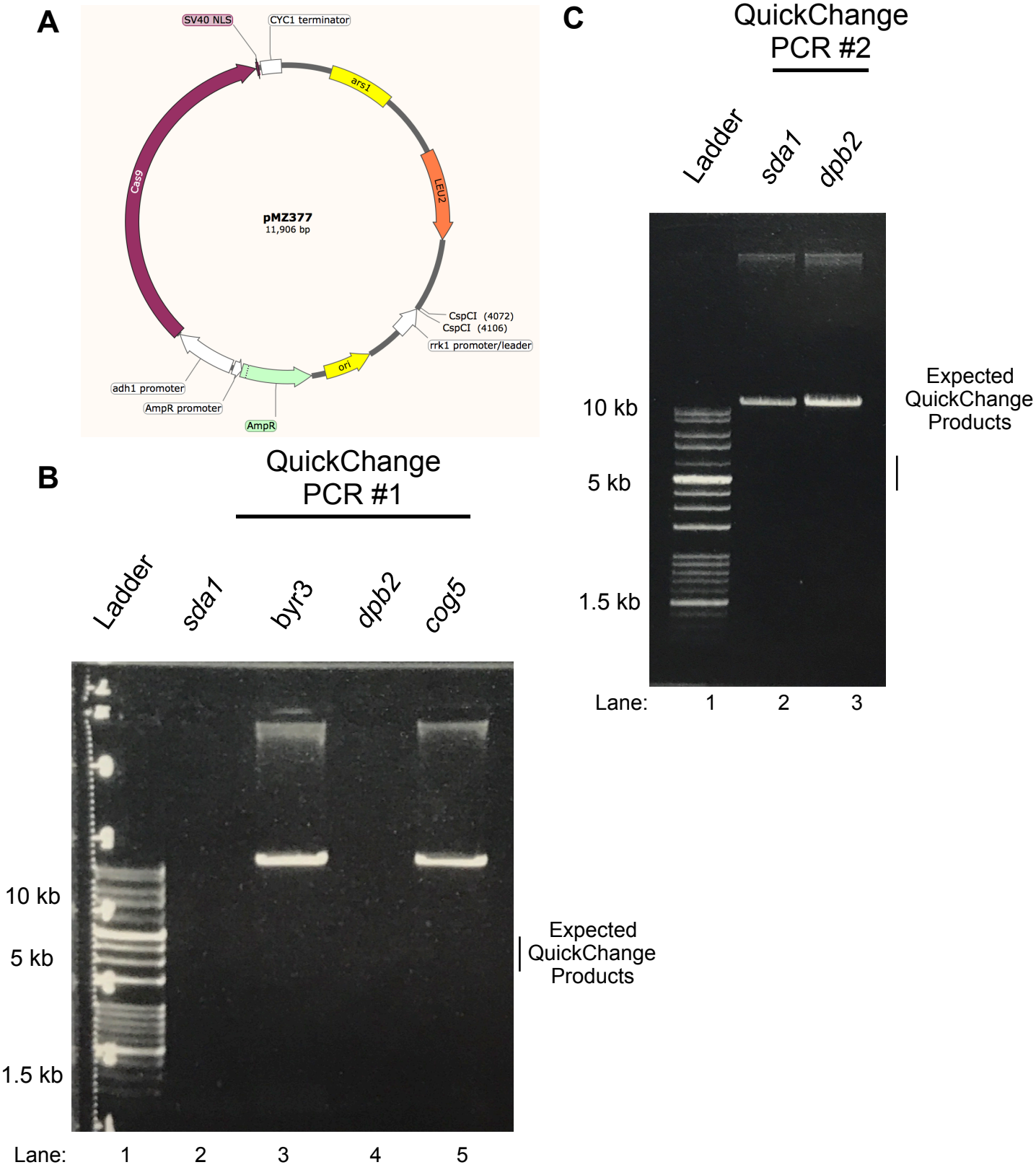

Figure 3. CRISPR/Cas9 Plasmid sgRNA QuickChange PCR with pMZ377. (**A**) Plasmid map from Addgene of pMZ377, a CRISPR/Cas9 plasmid designed for *S. pombe* containing the *leu2+* marker. (**B**) QuickChange PCR of *sda1+* (lane 2), *byr3+* (lane 3), *dpb2+* (lane 4), and *cog5+* (lane 5) sgRNA inserts. The QuickChange PCR protocol was performed according to the optimized reaction of figure 2B with 1 ng of sgRNA plasmid. Lane 1 contains the 10 kilobase VersaLadder. (**C**) The QuickChange PCR reaction was optimized to obtain results for the *sda1+* (lane 2) and *dpb2+* (lane 3) sgRNA inserts by utilizing 5 ng of pMZ377 template plasmid. Lane 1 contains the 10 kilobase VersaLadder.

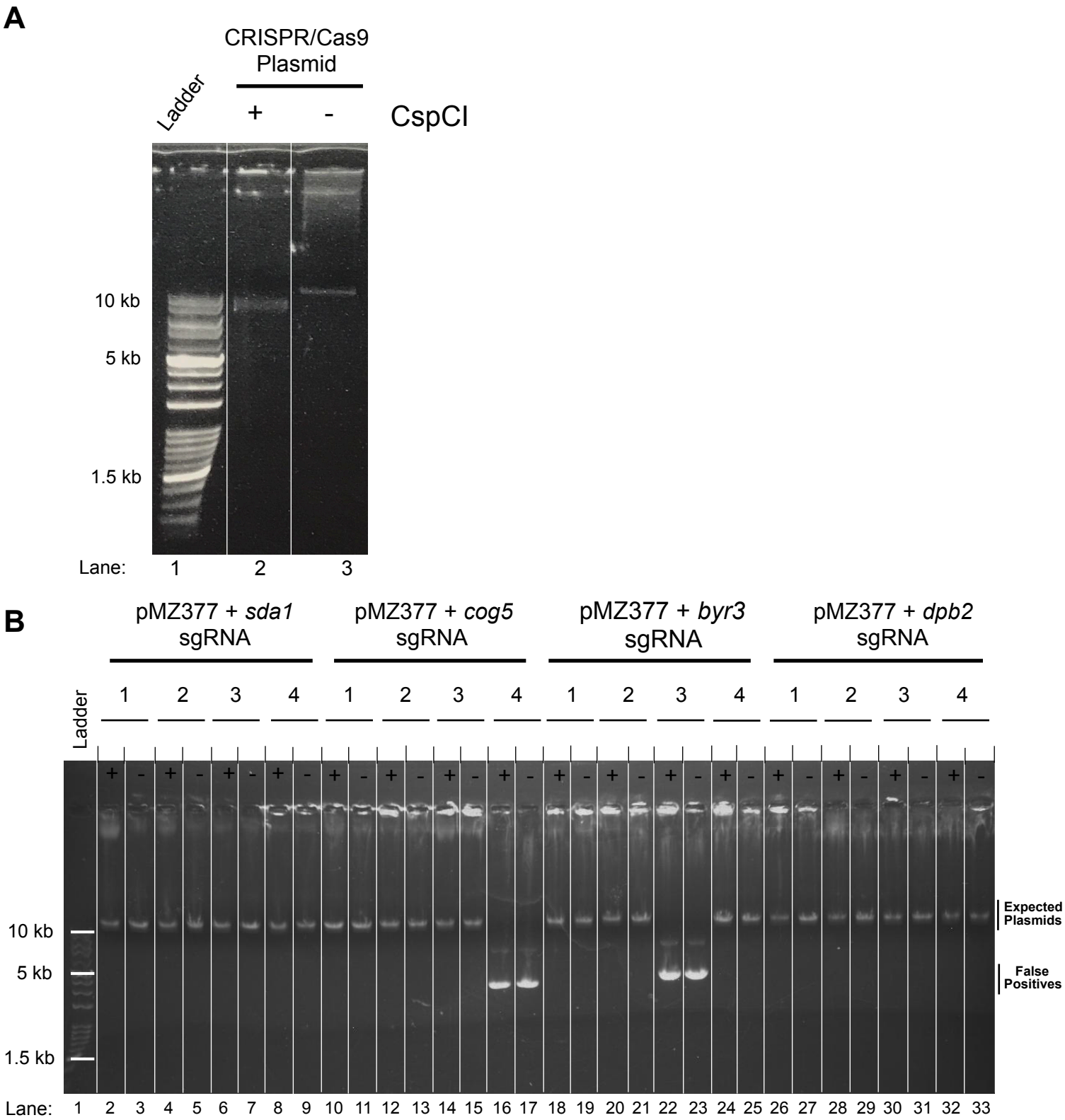

Figure 4. Confirming QuickChange PCR Results with Restriction Enzyme Digestion. (**A**) Restriction enzyme digest of purified CRISRP/Cas9 template plasmid. Lane 1 contains the 10 kb VersaLadder, Lane 2 contains the plasmid incubated with CspCI, and Lane 3 contains the uncut plasmid. Plasmids were incubated at 30º C for one hour with restriction enzyme (+) or in restriction enzyme buffer (-). (**B**) Restriction enzyme digest of QuickChange sgRNA PCR products for the *sda1*+, *cog5*+, *byr3*+, and *dpb2*+ sgRNA inserts. Lane 1 contains the 10 kb VersaLadder. An uncut plasmids (-) were run against plasmids that were treated with the CspCI restriction enzyme (+). Plasmids that exhibited the incorrect length were determined to be false positives. Isolated plasmids from each sample were incubated at 37º C for one hour with CspCI restriction enzyme (+) or with restriction enzyme buffer (-).

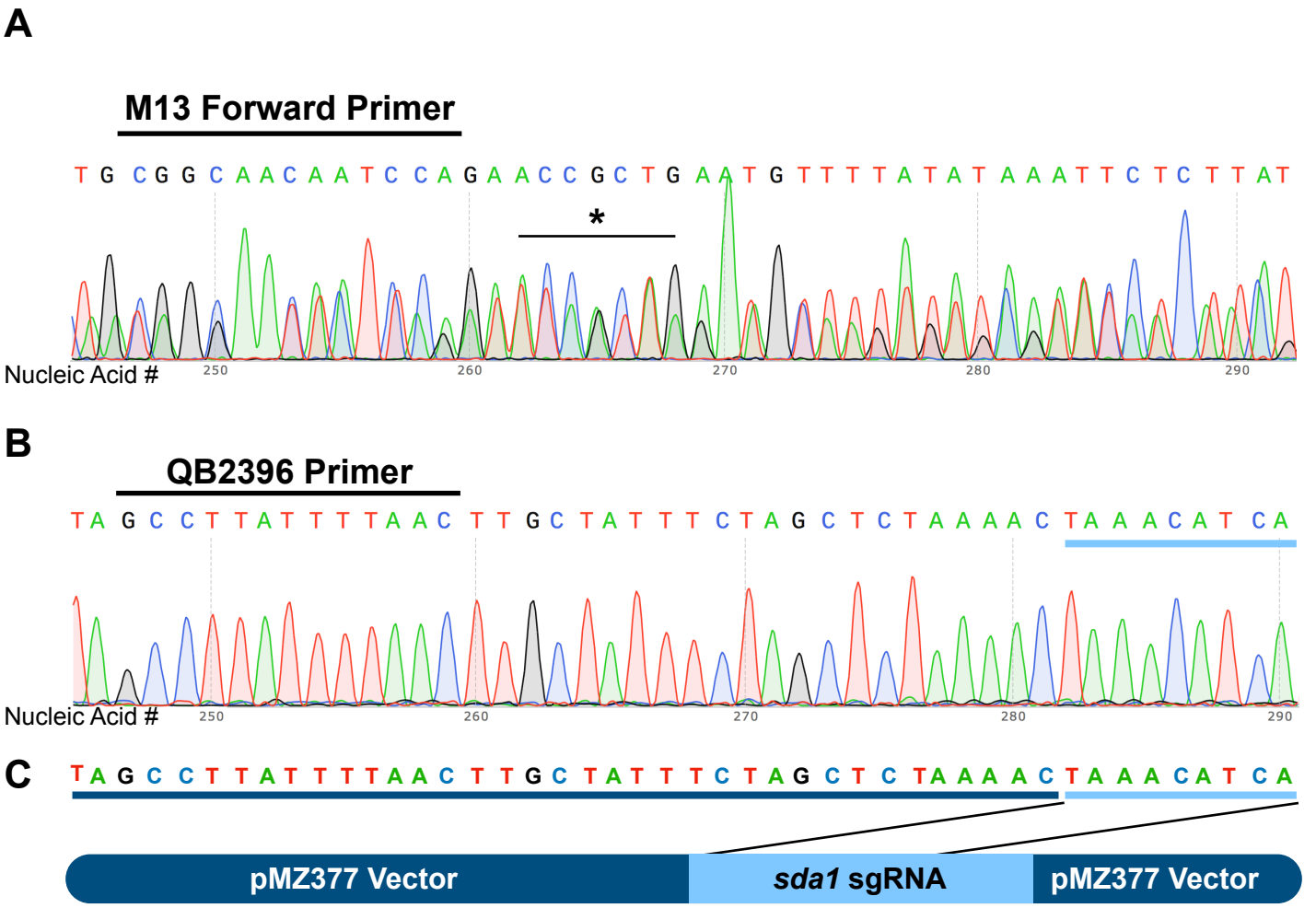

Figure 5. Sequencing Results from *sda1*+ sgRNA Samples. (**A**) Sequencing read outs from the *sda1* QuickChange PCR protocol with the M13 forward sequencing primer between nucleic acid residue #242 and nucleic acid residue #292. Sequencing results were returned with inconclusive results due to the presence of multiple peaks. Representative area of multiple peaks (asterisk). (**B**) Sequencing results from the CRISPR/Cas9 plasmid contain the *sda1*+ sgRNA that were resent for sequencing with the QB2396 primer. The sequencing window, nucleic acid residues #242 to nucleic acid residue #292 contains a portion of the sgRNA insert (blue bar). (**C**) The sequencing results of *sda1* CRISPR/Cas9 plasmids align with the insertion site on the pMZ377 vector and match the sequence of the *sda1*+ sgRNA primer sequence.

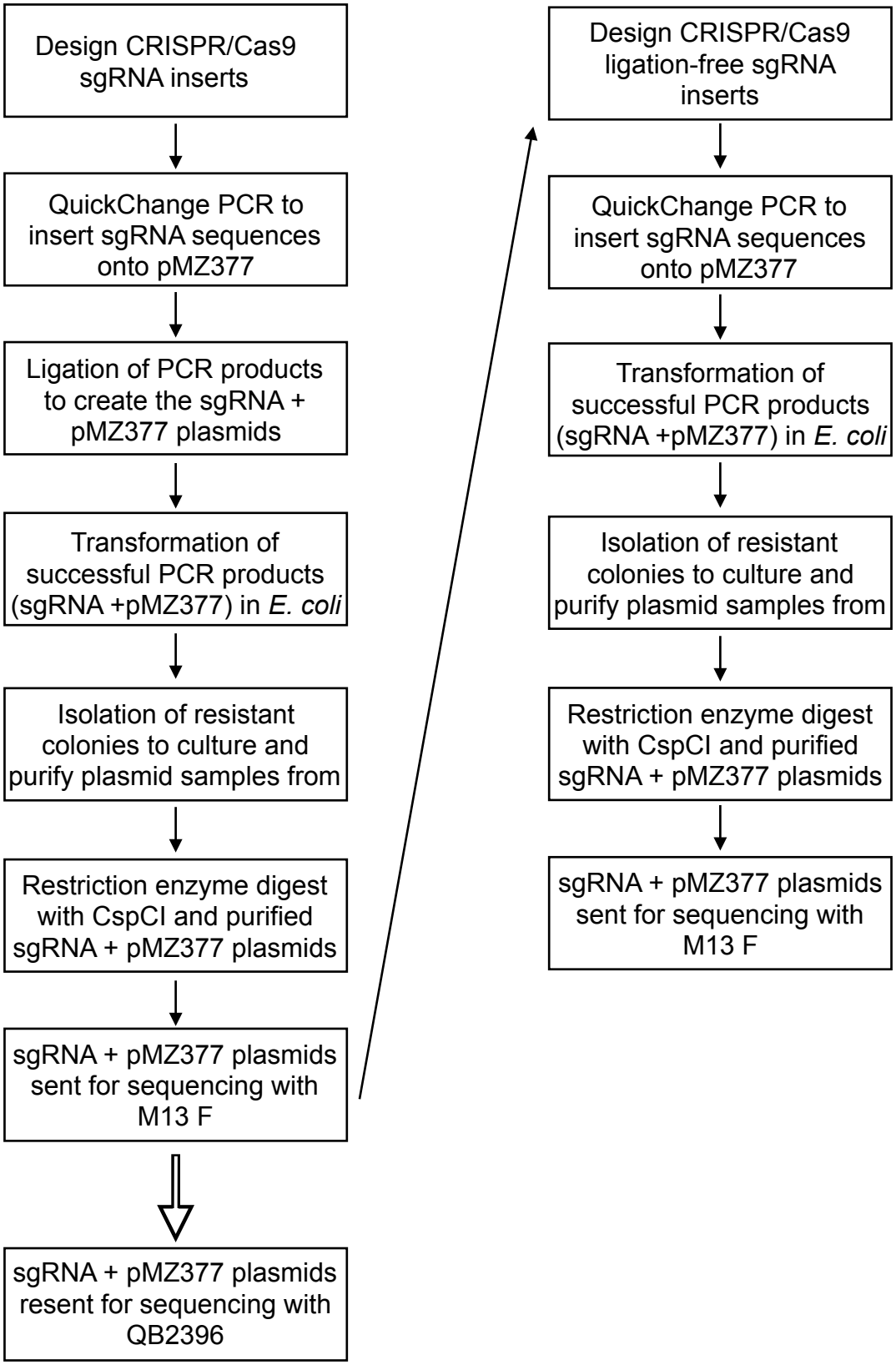

Figure 6. Flow Chart of CRISPR/Cas9 Methodology. Left. Initial CRISPR/Cas9 sgRNA inserts were designed and cloned into vectors with a protocol that required ligation of the final PCR product. Plasmids were sent in 10 ng/μL aliquots and stored at -80º C. Right. CRISPR/Cas9 ligation-free method was performed after sequencing results from the method requiring ligation were returned with inconclusive results with the M13 forward primer. Plasmids were sent for sequencing with the M13 forward primer at 10 ng/μL aliquots and stored at -80º C. After inconclusive sequencing results were returned with the M13 forward primer, the QB2396 primer was selected and successfully utilized for sequencing of pMZ377 plasmids with sgRNA inserts.

Work Cited:

1. Dillon, N. Heterochromatin structure and function. *Biology of the Cell* **96,** 631–637 (2004).
2. Doudna, J. A. & Charpentier, E. The new frontier of genome engineering with CRISPR-Cas9. *Science* **346,** 1258096 (2014).
3. Garcia, J. F., Al-Sady, B. & Madhani, H. D. Intrinsic Toxicity of Unchecked Heterochromatin Spread Is Suppressed by Redundant Chromatin Boundary Functions in Schizosacchromyces pombe. *G3 (Bethesda)* **5,** 1453–1461 (2015).
4. Grewal, S. I. S. & Jia, S. Heterochromatin revisited. *Nat. Rev. Genet.* **8,** 35–46 (2007).
5. Grewal, S. I. S. & Moazed, D. Heterochromatin and Epigenetic Control of Gene Expression. *Science* **301,** 798–802 (2003).
6. Haldar, S., Saini, A., Nanda, J. S., Saini, S. & Singh, J. Role of Swi6/HP1 Self-association-mediated Recruitment of Clr4/Suv39 in Establishment and Maintenance of Heterochromatin in Fission Yeast. *J. Biol. Chem.* **286,** 9308–9320 (2011).
7. Hay, R. T. SUMO: A History of Modification. *Molecular Cell* **18,** 1–12 (2005).
8. Hiraga, S., Botsios, S., Donze, D. & Donaldson, A. D. TFIIIC localizes budding yeast ETC sites to the nuclear periphery. *Mol Biol Cell* **23,** 2741–2754 (2012).
9. Isaac, S. *et al.* Interaction of Epe1 with the heterochromatin assembly pathway in Schizosaccharomyces pombe. *Genetics* **175,** 1549–1560 (2007).
10. Johnson, L. M., Cao, X. & Jacobsen, S. E. Interplay between Two Epigenetic Marks: DNA Methylation and Histone H3 Lysine 9 Methylation. *Current Biology* **12,** 1360–1367 (2002).
11. Kirkland, J. G., Raab, J. R. & Kamakaka, R. T. TFIIIC Bound DNA Elements in Nuclear Organization and Insulation. *Biochim Biophys Acta* **1829,** 418–424 (2013).
12. Klose, R. J., Kallin, E. M. & Zhang, Y. JmjC-domain-containing proteins and histone demethylation. *Nat Rev Genet* **7,** 715–727 (2006).
13. Lomberk, G., Wallrath, L. & Urrutia, R. The Heterochromatin Protein 1 family. *Genome Biol* **7,** 228 (2006).
14. Lorentz, A., Ostermann, K., Fleck, O. & Schmidt, H. Switching gene swi6, involved in repression of silent mating-type loci in fission yeast, encodes a homologue of chromatin-associated proteins from Drosophila and mammals. *Gene* **143,** 139–143 (1994).
15. Mesa, K. Essential Cell Biology. *Yale J Biol Med* **88,** 100–101 (2015).
16. Mizuguchi, T., Barrowman, J. & Grewal, S. I. S. Chromosome domain architecture and dynamic organization of the fission yeast genome. *FEBS Lett* **589,** 2975–2986 (2015).
17. Noma, K., Cam, H. P., Maraia, R. J. & Grewal, S. I. S. A Role for TFIIIC Transcription Factor Complex in Genome Organization. *Cell* **125,** 859–872 (2006).
18. Rodríguez-López, M. *et al.* A CRISPR/Cas9-based method and primer design tool for seamless genome editing in fission yeast. *Wellcome Open Research* **1,** 19 (2017).
19. Scott, K. C., Merrett, S. L. & Willard, H. F. A heterochromatin barrier partitions the fission yeast centromere into discrete chromatin domains. *Curr. Biol.* **16,** 119–129 (2006).

20. Smith, B. C. & Denu, J. M. Chemical mechanisms of histone lysine and arginine modifications. *Biochimica et Biophysica Acta (BBA) - Gene Regulatory Mechanisms* **1789,** 45–57 (2009).
21. Talbert, P. B. & Henikoff, S. Spreading of silent chromatin: inaction at a distance. *Nat Rev Genet* **7,** 793–803 (2006).
22. Trewick, S. C., Minc, E., Antonelli, R., Urano, T. & Allshire, R. C. The JmjC domain protein Epe1 prevents unregulated assembly and disassembly of heterochromatin. *The EMBO Journal* **26,** 4670–4682 (2007).
23. Wang, J., Lawry, S. T., Cohen, A. L. & Jia, S. Chromosome boundary elements and regulation of heterochromatin spreading. *Cell Mol Life Sci* **71,** 4841–4852 (2014).
24. Zhang, K., Mosch, K., Fischle, W. & Grewal, S. I. S. Roles of the Clr4 methyltransferase complex in nucleation, spreading and maintenance of heterochromatin. *Nat. Struct. Mol. Biol.* **15,** 381–388 (2008).
25. Zofall, M. & Grewal, S. I. S. Swi6/HP1 Recruits a JmjC Domain Protein to Facilitate Transcription of Heterochromatic Repeats. *Molecular Cell* **22,** 681–692 (2006).